Sustainable Cities and Society 73 (2021) 103098

Contents lists available at ScienceDirect

Sustainable Cities and Society

journal homepage: www.elsevier.com/locate/scs

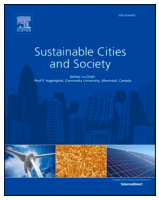

A vast increase in heat exposure in the 21st century is driven by global warming and urban population growth

Tamir Klein [a,+,*], William R.L. Anderegg [b,+]

[a] Department of Plant and Environmental Sciences, Weizmann Institute of Science, Rehovot 76100, Israel
[b] School of Biological Sciences, University of Utah, Salt Lake City, UT, USA

ARTICLE INFO

Keywords:
Climate change
Population growth
Heat exposure
Global warming
India
Africa

ABSTRACT

Over the 21st century, human-caused climate change is projected to vastly increase the occurrence of severe heat, which has deleterious health, economic, and societal impacts. Over the same period, global human population is expected to increase from 7.8 to 10.9 billion, placing more people in harm's way. Here, we combine projections of sustained heat from climate models with spatially explicit population projection scenarios. We find that: (1) by 2090, high climate change and population growth scenarios show a ~5-, ~10-, and ~100–1000-fold increase in the population exposed to a mean hottest monthly temperature of 30 °C, 35 °C, and 40 °C, respectively; (2) globally, population growth, warming, and their interaction, are the major drivers for the increase in exposure at milder, harsher, and extreme, temperatures, respectively; and (3) differences between population growth scenarios show that policy can potentially reduce the level of increase in exposure by up to 70%. Based on our analyses, the major driver for the increased heat exposure is the dangerous combination between global warming and population growth in already-warm cities in regions like Africa, India, and the Middle East.

1. Introduction

Anthropogenic climate change has already increased mean global temperature from that of the 1950s by ~1.0 °C, and projections indicate that another 2.5–4 °C increase is possible by the end of the 21st century in high emissions scenarios (Hansen, Sato, & Ruedy, 2012, IPCC 2014: Pachauri et al., 2014). Temperature projections made by models between 1970 and 2007 and actual temperatures have recently shown that the high-end projections matched the observations quite well (Hausfather, Drake, Abbott, & Schmidt, 2020). Temperatures related with extreme heat rise faster than average temperatures because climate change drives an increase in both the mean and the variance of temperatures (Field, Barros, Stocker, & Dahe, 2012). Thus, increasing occurrences of severe heat stress have been widely documented and attributed to anthropogenic forcing of the climate (Diffenbaugh et al. 2011; Field, Barros, Stocker, & Dahe, 2012) and future projections indicate still larger increases in occurrence of severe heat conditions (Jones et al., 2015; Jones, Tebaldi, O'Neill, Oleson, & Gao, 2018; Mora et al., 2017; Sherwood & Huber 2010; Xu, Kohler, Lenton, Svenning, & Scheffer, 2020). Extreme heat events have numerous harmful consequences on ecosystems and society. For example, the 2003 heatwave in Europe killed an estimated 70,000 people (Robine et al. 2008). Further warming is expected to decrease worker productivity during hot months of the year (IPCC 2018: Hoegh-Guldberg et al., 2018).

Human populations have also increased rapidly starting in the 1950s (2.5 billion people at the time), reaching 7.8 billion people in 2020, and are projected to increase to 10.9 billion by the end of the 21st century in a mid-range scenario (UN 2019). Similar to temperatures, projections made decades ago (Bulatao, Bos, Stephens, & Vu, 1990; Frejka, 1981; Vu, 1985) proved remarkably accurate. Crucially, human population is unequally distributed across the globe, with the majority of population residing in moderate precipitation (500–1500 mm year^{-1}) and relatively warm regions (mean annual temperature > 15 °C) (Sherwood & Huber 2010; Small & Cohen 2004; Xu et al., 2020). Governments and international organizations have worked to address both climate change and population growth, albeit with relatively limited success to date (Bongaarts & O'Neill, 2018). Recent studies have emphasized the substantial benefits of considering population efforts alongside climate policies (Ahmadalipour, Moradkhani, Castelletti, & Magliocca, 2019; Rohat, Flacke, Dosio, Dao, & van Maarseveen, 2019). In particular, the interaction between changing populations and climate change is crucial because growing populations may place more people "in harm's way"

* Corresponding author.
E-mail address: tamir.klein@weizmann.ac.il (T. Klein).
+ These authors contributed equally to the study.

https://doi.org/10.1016/j.scs.2021.103098
Received 9 January 2021; Received in revised form 10 June 2021; Accepted 12 June 2021
Available online 16 June 2021

for climate impacts, as well as influencing adaptation capacity.

The heterogeneity of the spatial distribution of human population is also expressed in the congregation into dense metropolitan areas. In 2007, for the first time in human history, the share of urban population increased over that of rural population. This trend continues to intensify, and according to UN projections, by 2050, 68% of the world population is projected to live in urban areas. In turn, this means that the grand challenge of the combined increase in global population size and high temperatures is exacerbated with the urban challenges of increased density and the urban heat island (Peng et al. 2012). Cities are typically warmer than their adjacent rural areas, and, due to their interference with the natural surface-atmosphere heat balance, have higher rates of extreme hot nights (McCarthy, Best, & Betts, 2010). For example, urban areas in a city in India were up to 2.1 and 2.3 ºC warmer than suburban areas during day and night, respectively (Borbora & Das, 2014).

While recent literature has focused on historical and projected changes in heatwaves (Jones et al., 2015; Jones et al., 2018; Mora et al., 2017; Sherwood & Huber 2010), a detailed assessment of spatiotemporal patterns in population exposure to severe heat across temperature thresholds, population scenarios, and climate scenarios from multi-model ensemble projections is urgently needed. An estimated ~30% of the world's population is currently exposed to climatic conditions conducive of heat-related mortality for at least 20 days a year (Mora et al., 2017). Moreover, this percentage is projected to increase to 48–74%, depending on the greenhouse gas emission scenario. Recent studies show a 4–6 fold increase in US population exposure to heat extremes (temperatures higher than 35 ºC) toward the end of the century (Jones et al., 2015), and a significant increase in the exposure to these events on a global scale (Jones et al., 2018). Here, we leverage recent spatially explicit population projection scenarios and Earth system model output to examine population exposure to extreme heat. We ask: (1) how does the change in population exposure to heat between 2010 and 2090 vary with temperature threshold? (2) What are the spatial and temporal patterns of severe heat exposure? And (3) what are the relative drivers of change in exposure among climate change alone, population growth alone, and their interaction?

2. Methodology

2.1. Datasets

We used spatially-explicit population projections for four shared socioeconomic pathway (SSP) scenarios that bracket the full range of population and climate changes expected in the 21st century (Jones & O'Neill 2016). The population data can be downloaded from the National Center for Atmospheric Research (NCAR) website and data portal (https://www.cgd.ucar.edu/iam/modeling/spatial-population-scenarios.html). The spatial projections are based on a parameterized gravity-based downscaling model that projects changes in rural and urban populations at sub-national grid cells, while accounting for both geographic characteristics of the landscape and protected areas. The model was calibrated to reproduce observed historical changes and is consistent both with historical trends and broad-scale SSP patterns. We chose that dataset because it provides spatially-explicit population projections at a spatial resolution relevant to comparing to climate model output in CMIP6. The uncertainties and limitations of those projections are discussed in the Discussion section of Jones and O'Neill (2016). These projections provide urban, rural, and total population at 0.125 ° spatial resolution globally and decadal resolution temporally from 2010–2100. In the analyses presented here, we focused on the total population in each grid cell and the time periods of 2010 and 2090. These specific years were chosen to represent early and late 21st century, for which reliable climate and population projections are available. While SSP1 assumes that the world shifts toward a more sustainable path, SSP3 assumes that concerns about competition and security among nations prevent such a desired shift. SSP2 indicates a middle solution between the two scenarios, and SSP5 assumes that technological innovation allows for climate change adaptation, with little mitigation. For simplicity, we chose to exclude SSP4 (Inequality; Riahi et al., 2017), since its projections of population growth and environmental impacts lie in between those produced by other scenarios. Therefore, the range of possible responses was covered by the "Tier 1″ scenarios, i.e. SSP1, 2, 3, and 5. SSP1 is generally consistent with the radiative concentration pathway (RCP) 2.6 or 1.9, SSP2 with RCP 4.5, SSP3 with a 7.0 W/m^2 change by 2100, and SSP5 with RCP 8.5 (Van Vuuren & Carter 2014).

We used climate projections from seven climate/Earth system models in the Coupled Model Intercomparison Project Phase 6 (CMIP6; Eyring et al., 2016) (Table 1). These models were chosen because they provided monthly temperature projections for the historical period studied here. We downloaded the monthly average surface air temperature ('tas') for all climate models and all SSPs, comprising historical data from 1850–2014 and future projections from 2015–2100. We took a subset of the years 1995–2014 for the historical period and 2081–2100 for future projections to capture inter-annual variability around the focal population estimates from 2010 and 2090.

2.2. Analyses

We regridded all climate model output and population projections to a common 1×1 ° grid using resampling via bilinear interpolations, ensuring that the distributions of population and hottest temperatures were preserved after resampling, in order to facilitate direct comparisons between temperatures and population. Since the majority of human population is living in clustered urban and rural settlements, we tested that re-projecting both the population and climate datasets to 1 ° did not bias the results. To do so, we calculated the population exposed across various temperature thresholds in SSP3 in the 2090s via the resampling method we used for all other analyses (x-axis of Fig. S1) and then calculated exposure using the raw resolution of the population data (0.125 ° grid; y-axis of Fig. S1). The two were almost identical (less than 1% difference). The r^2 between the two is >0.999 and the slope between them was 1.006. It is therefore very unlikely that our resampling had any major impact on the results.

For each grid cell, year, and climate model combination, we extracted the hottest month of the year. Severe heat can be quantified in a wide variety of ways, including percentile-based approaches and absolute temperature thresholds (Rohat et al., 2019; Sherwood & Huber, 2010). We chose the absolute temperature of the hottest month because we are focused on average exposure to severe heat, rather than individual hot spells or heatwaves. In both 2010 and 2090, we calculated the total population globally experiencing a hottest month above a given temperature threshold (e.g. 35 ºC) and estimated the standard deviation via the variation across the 20 year windows within a climate model and across all seven climate models. We then calculated the percentage change in population exposed by comparing 2090 population exposure to 2010 exposure.

We conducted an additional analysis to examine the relative importance of climate change alone, population growth alone, and the interaction between the two in driving the change in exposure. We estimated the climate-alone contribution by calculating the change in population exposure at a given temperature threshold using 2081–2100

Table 1
Climate models included in the analysis.

Research group	Climate model
Beijing Climate Center (BCC)	CSM2-MR
Chinese Academy of Meteorological Sciences (CAMS)	CSM1–0
National Center for Atmospheric Research (NCAR)	CESM2
Canadian centre for Climate Modeling and Analysis	CanESM5
Institut Pierre Simon Laplace (IPSL)	CM6A-LR
Japan Agency for Marine-Earth Science and Technology	MIROC6
Meteorological Research Institute (MRI)	ESM2–0

climate projections overlaid on 2010 population levels. We estimated the population-alone contribution by tabulating the 1995–2014 climate data overlaid on 2090 population levels. Finally, we estimated the interaction of the two as the total change in population exposure minus the sum of the climate-alone and population-alone changes. This interaction term aims to provide an estimate of how much the change in exposure is driven by climate and population changes that are disproportionately co-located.

Finally, to calculate changes in population heat exposure of the world's largest cities, we used city-specific population estimates reported in Hoornweg and Pope (2017) for 2010 and 2100. That analysis included the 101 largest cities at each of the time points, starting with Addis Ababa in 2010 (Ethiopia; 3.4 million people in 2010), and with Rawalpindi in 2100 (Pakistan; 7.9 million people projected in 2100).

All analyses were conducted in the R statistical environment (R Core Development Team 2012). NetCDF analyses drew upon the 'RNetCDF' package (Michna and Woods 2013). Spatial analyses were conducted using the 'raster' package and plotted via the 'rworldmap' (Hijmans et al. 2014; South, 2011). Violin plots were made using the 'plotrix' package (Lemon, 2006).

3. Results

We first examined the population globally that experiences different mean temperatures during the hottest month of the year in 2010, 2050 and 2090 in a high emissions/high population-growth scenario (Fig. 1). We chose this metric as an indicator of seasonal, long-term heat exposure, as opposed to shorter-term heatwave episodes. The distribution is expected to shift to the right (increasingly higher temperatures) due to global warming. Simultaneously, this distribution is expected to shift upwards (an increasingly larger number of people) due to both climate change and population growth. In 2010, less than 30% of world population (2 billion people; Fig. 1) was exposed to a mean temperature of the hottest month of 30 ºC or higher. Strikingly, in 2050 and 2090, this number increases to almost 5 and 9 billion people, respectively, in this scenario, the latter number being more than the current total world population. Out of these 9 billion heat-exposed people, more than 3 billion people will be exposed to a mean hottest month temperature of 36 ºC or higher. Under very humid conditions, this temperature is above

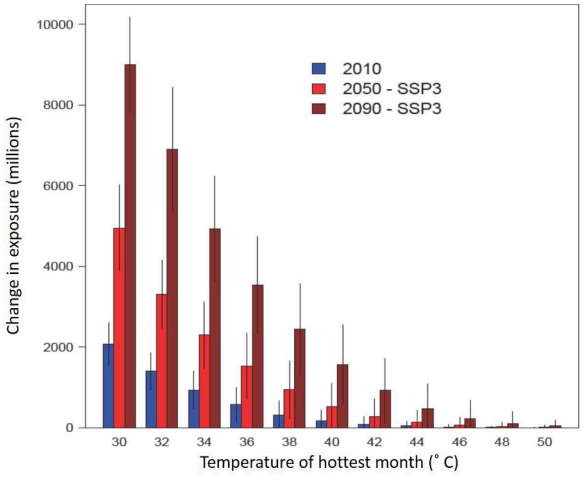

Fig. 1. Additional billions of people are projected to be exposed to a mean hottest month temperature of 30–38 ºC in 2090 than in 2010. The distribution of world population by mean temperature of hottest month for 2010, 2050 and 2090 (x-axis values are thresholds). Projection is based on the shared socioeconomic pathway (SSP) scenario 3 (regional rivalry) with radiative forcing of 7.0 W m^{-2}. Error bars are ± 1 standard deviation across seven Earth system models and climate data from 1995–2014, 2041–2060 and 2081–2100 for 2010, 2050, and 2090 population levels, respectively.

the physiological wet-bulb threshold of 35 ºC, where removal of metabolic heat becomes impossible. In addition, mean hottest month temperatures of 28–35 ºC mean that average high temperatures are 35 ºC in relatively humid sites like Kolkata (India) and Cairo (Egypt), and can reach 40–44 ºC in continental sites like Delhi (India) and Baghdad (Iraq).

The spatial distribution of the increase in heat exposure reveals key geographic hotspots (Fig. 2). Exposure to a hottest month temperature of 30 ºC is projected to increase in 2090 across most low- and mid-latitude regions. Our analysis shows that the majority of these heat-exposed people will be in regions like India, Bangladesh, Indonesia, The Philippines, Nigeria, the Middle East, and Eastern China (Fig. 2A). The largest impact will likely be in large urban areas within these countries (e.g. Delhi, Baghdad, and Cairo). Looking at extreme heat exposure, the hotspots in India, Nigeria, and Iraq, are further highlighted with millions of people exposed to hottest month temperatures of 35 ºC (Fig. 2B). Bangladesh rises as the largest extreme heat exposure hotspot globally. We note that some of the moderate exposure increases identified in the maps are localized to sparsely populated regions, such as arid regions in Africa (Sahara), Asia (Arabian Desert) and Australia. Unlike the focal regions identified above (India, Bangladesh, Nigeria, the Middle East), increases in these arid regions are low in absolute numbers of population exposed.

We next examined the change in population heat exposure as the percent change from 2010 to 2090 across multiple future population and climate scenarios. We found increases in exposure to hottest month temperature of 30 ºC or higher of around 100% (i.e., a doubling in the number of heat-exposed people). However, increased exposure to temperatures of 35 ºC and 40 ºC was roughly around 300% and 1000%, respectively. The exposure to heat varied substantially across four different shared socioeconomic pathways (SSPs). Briefly, SSP1 assumes that the world shifts toward a more sustainable path and exhibits low population growth and low levels of climate change. By contrast, SSP3 assumes that concerns about competition and security among nations prevent such a shift and climate change and population growth proceed rapidly. SSP 2 indicates a middle-of-the-road path between SSP1 and SSP3, and SSP5 assumes that technological innovation allows for low population growth levels and climate change adaptation, with little mitigation leading to large levels of climate change. We observed a consistent pattern among SSP1, 2, and 3, in terms of the increase in population heat exposure, with SSP5 producing lower exposure than projected by SSP3, but similar or higher than SSP2 (Fig. 3).

We next partitioned the change in population exposure to heat among the effects of climate change, population growth, and their interaction. We repeated this process for the four SSPs. Among the three factors (climate change, population growth, and their interaction), climate change had the higher effect in three of the four SSPs (Fig. 4). This pattern was most obvious in SSP5, due to the lack of mitigation, in turn inducing the warming, and relatively limited population growth (SSP5 actually predicts a lower global population in 2090 than in 2010). In contrast, SSP3 results showed a higher role for population growth than climate change.

Specifically, at temperatures of 36 ºC or higher, the interaction between population growth and warming had a major effect on the increase in the number of people being exposed to heat, more than that of each factor alone. Considering that SSP3 presents the most direct continuation of present-day trajectories of both climate and population, this result suggests that most of the increase in population exposure to temperatures of 36 ºC or higher relates to rapid population growth in warm locations. Overall, major differences in the level of exposure emerged among SSPs (Fig. 4). At the extremes, the 4-fold increase in population exposure to hottest month temperatures of 30 ºC or higher, projected by SSP3 (Fig. 1), was merely a 45% increase in SSP1.

The expected increase in population heat exposure during this century is clearly visible in and amplified by the changes to the list of the world's largest cities. In 2010, the ten most populated cities represented a mixture of high- and low-latitudes across Asia and the Americas

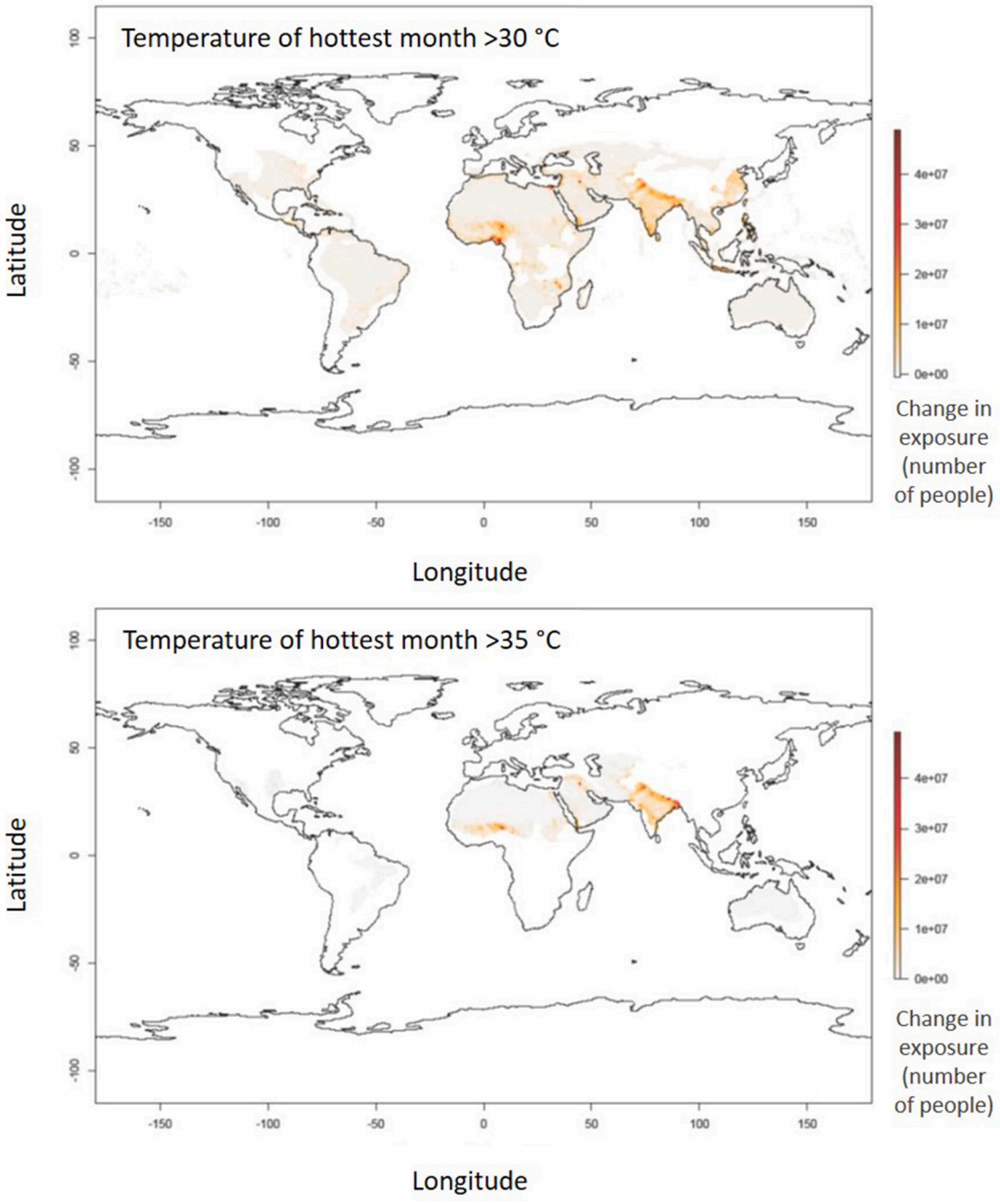

Fig. 2. Increased exposure to extreme heat is prevalent across low-mid latitudes. Change in exposure (number of people) between 2081–2100 versus 1995–2014 of the mean temperature in the hottest month of the year in the shared socioeconomic pathway 3 (SSP3) scenario (regional rivalry) for two temperature thresholds.

(Table 2). This meant that the total of 200 million people residing in these cities were mostly exposed to mean daily temperatures ≤30 °C (Delhi, India, being an exception with 33.2 °C). In contrast, the 2100 list is composed of cities of unprecedented size in tropical Africa and Asia, led by Lagos (Nigeria) with a projected population of 60 or 100 million people, according to SSP1 or SSP3, respectively. The combined effects of global warming and the geographical shift away from higher, cooler, latitudes, meant that in 2100, seven of the ten cities had mean daily temperatures >30 °C. Again, Delhi, India, was the hottest, with mean daily temperature of the hottest month of 36.7 °C.

Comparing the heat exposure in the world's largest cities in 2010 vs. 2100 indicated hotter conditions for larger populations in e.g., Mumbai and Kolkata (India). Moreover, in Dhaka (Bangladesh), 15 million people that were not regularly exposed to extreme heat in 2010, shifted to temperatures >30 °C, while affecting a three-fold larger population (Table 2). Similar temperature exceedances were projected for some African cities, that were absent from the 2010 list altogether, by 2100. For example, Lagos had 10.6 people in 2010, with mean daily temperature of the hottest month of 28.5 °C (data not shown), and is expected to grow 6–10 fold, with mean daily temperature of the hottest month of 31.5 °C. Karachi in Pakistan is another example, being a 13.0 million people city with a temperature of 31.8 °C in 2010, and growing 3–4 fold with a temperature of 34.8 °C in 2100. In the Middle East, cities like Cairo (Egypt) and Baghdad (Iraq) should grow from 12.5 to 40.5 million people and from 5.9 to 34.1 million people during this century. Mean daily temperature of the hottest month should increase from 28.2 to 31.2

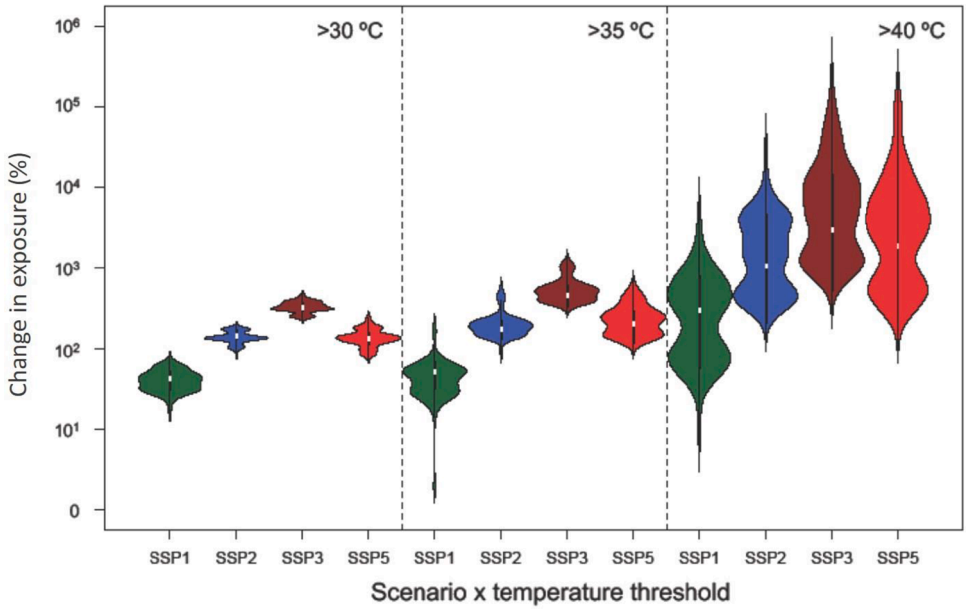

Fig. 3. A 100–1000% increase in the population exposed to extreme heat by the 2090s. Percent change between 2081–2100 versus 1995–2014 of people exposed to a given mean temperature threshold during the hottest month of the year for four shared socioeconomic pathway (SSP) scenarios of population growth and climate change: SSP1, sustainability; SSP2, middle of the road; SSP3, regional rivalry; and SSP5, fossil-fueled development.

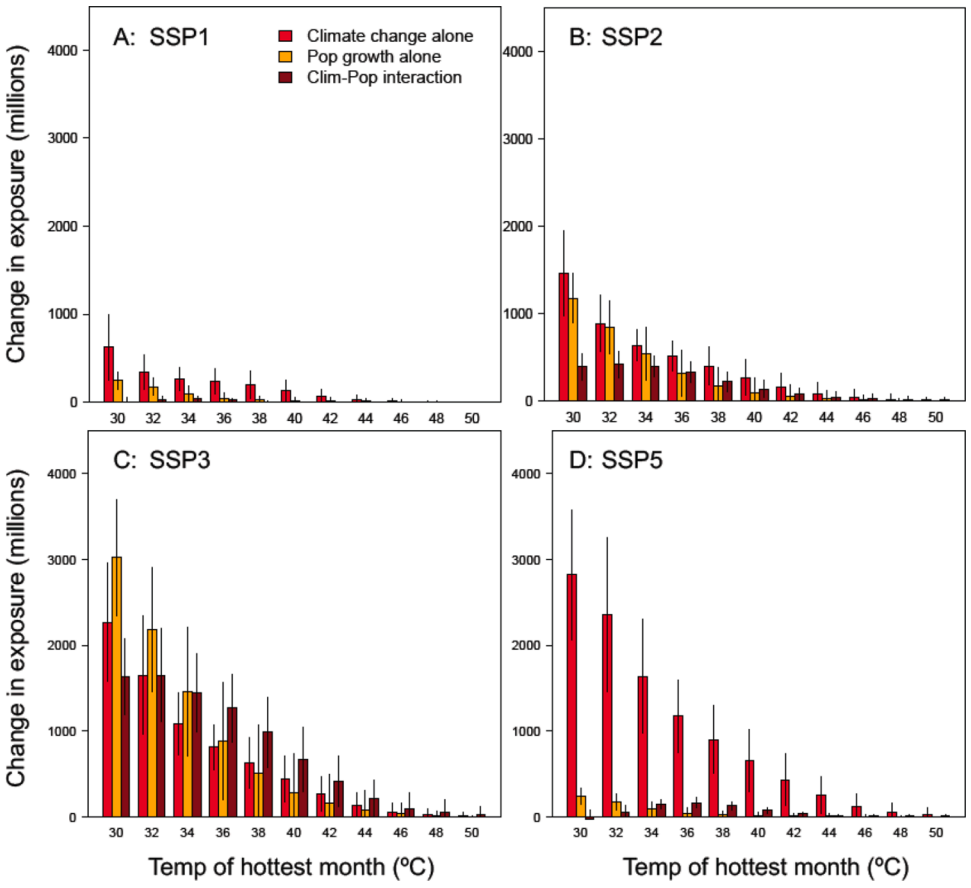

Fig. 4. Climate change and population growth interact to expose hundreds of millions to heat by the 2090s. Change in global exposure (millions of people) between 2081–2100 versus 1995–2014 as a function of climate change alone (red), population growth alone (yellow), and the interaction between climate change and population growth (dark red) for shared socioeconomic pathway (SSP): (A) SSP1, sustainability; (B) SSP2, middle of the road; (C) SSP3, regional rivalry; and (D) SSP5, fossil-fueled development. X-axis values are temperature thresholds. Error bars present the mean ±1 standard deviation across the seven Earth system models analyzed.

°C in Cairo, and from 34.8 to a staggering 38.3 °C in Baghdad. Overall, the population of the world's ten largest cities should increase from 200 million people with a mean hottest month temperature of 27.2 °C in 2010, to 440–580 million people with a mean hottest month temperature of 31.1 °C in 2100 (Table 2).

4. Discussion

Almost two decades ago, Cohen (2003) wrote: "Human choices, individual and collective, will have demographic effects, intentional or otherwise". Our analyses indicate that differences among scenarios –

Table 2
The world's largest cities (urban areas) by population (Pop.; millions) and their mean hottest monthly temperature (Temp.; ºC) in 2010 and in 2100, for the shared socioeconomic pathways SSP1 (sustainability) and SSP3 (regional rivalry).

	2010			2100	SSP1		2100	SSP3	
	City	Pop.	Temp.	City	Pop.	Temp.	City	Pop.	Temp.
1	Tokyo	36.1	25.5	Lagos	61.0	31.5	Lagos	100.2	31.5
2	Mexico city	20.1	20.0	Mumbai	52.3	33.5	Dar es Salaam	77.5	30.9
3	Mumbai	20.1	30.5	Kinshasa	48.8	29.9	Luanda	69.2	31.6
4	Beijing	19.6	26.5	Karachi	44.4	34.8	Karachi	52.9	34.8
5	Sao Paulo	19.6	23.2	Delhi	44.3	36.7	Mumbai	52.6	33.5
6	New York	19.4	24.7	Dar es Salaam	43.2	30.9	Kinshasa	50.8	29.9
7	Delhi	17.0	33.2	Dhaka	40.7	32.0	Mexico city	46.5	23.0
8	Shanghai	15.8	28.6	Kolkata	40.6	33.9	Dhaka	45.5	32.0
9	Kolkata	15.6	30.9	Nairobi	33.9	21.9	Delhi	44.6	36.7
10	Dhaka	14.8	29.0	Kampala	33.1	26.7	Lusaka	40.9	27.0
		Total	Mean		Total	Mean		Total	Mean
		198.1	27.2		442.3	31.2		580.7	31.1

controlled fundamentally by human actions on climate mitigation and demographic choices – have enormous leverage on the global population exposed to heat in the 21st century (Fig. 4). Comparisons between SSP1 and SSP3 (Figs 2, 4) provide evidence to the benefits of both climate and population policy changes. In the sustainable scenario (SSP1), population exposure to heat can be almost stabilized by the end of this century. We calculated that the 2010 population size exposed to a mean summer temperature of 30 ºC or higher (2 billion) may increase to ~3 billion in 2090 in SSP1, and ~9 billion in SSP3. These differences show that the combined effect of climate and demographic policy can potentially reduce the level of increase in exposure by up to 70%, which are 6 billion people. This policy-driven percent decrease persists for higher temperature thresholds. Differences between SSP3 and SSP5 are primarily due to different population growth scenarios, as both scenarios exhibit high levels of climate change.

How does our study differ from previous studies on population heat exposure? And how do our results compare with those? Two major parameters make our approach unique and robust. First, the metric of a mean hottest month temperature provides a good balance between focusing on heatwaves alone (Jones et al., 2015; Jones et al., 2018; Mora et al., 2017; Rohat et al., 2019; Sherwood & Huber 2010) on the one hand, and considering the mean annual temperature (Xu et al., 2020) on the other hand. Doing so, we offer a metric which better characterizes the overall heat exposure, regardless of the stochastic occurrence of extreme events. Moreover, unlike past studies that counted heat exposure by the term of person-days (Jones et al., 2015, 2018; Rohat et al., 2019), quantifying the exposure by the number of people per a given metric threshold yielded intuitive results. Second, we tested here the five SSPs, which was not done on a global scale before (e.g. Mora et al., 2017) and has only been done for African cities (Rohat et al., 2019). These two differences limit our ability to directly compare our results with those of previous studies. Still, some intriguing patterns emerge. The projection by Mora et al. (2017) of an increase in 'deadly heat' exposure from 30% to 74% of global population seems to correspond well with our projection of increase from ~2 to ~9 billion people (Fig. 1). The projection of Xu et al. (2020), based on mean annual temperature of 29 ºC probably relates to our hottest month threshold of 36 ºC, showing the very same increase from ~1% of global population, up to 3 billion people. Fold-changes were given in some studies, e.g. for population exposure to heatwave occurrence. The 4–6-fold increase projected for the USA (although only up to 2070; Jones et al., 2015) is dwarfed by the 20–52-fold increase projected for African cities (Rohat et al., 2019). Importantly, these projections for USA and Africa are in line with our respective predictions for the temperature thresholds of 30 ºC and 35–40 ºC, indicating 5-fold increase in the cooler, USA, case, and 10–100-fold increase in the warmer, Africa, case.

A key finding of our analyses is that the already-hot regions of the globe are those expecting the highest population increase. In the Middle East, millions of people living in cities like Baghdad, Tel Aviv and Cairo will be exposed to extreme heat on a seasonal basis (Fig. 2). For Africa, our observations (Fig. 2) are in line with recent projections that exposure to dangerous heat in African cities will increase 20–52 fold in 2090, depending on the scenario (Rohat et al., 2019). The interactions between population and climate are often quite complex. For example, population growth in sub-Saharan Africa may have offset climate-driven increase in woody vegetation, through increasing demands for agricultural land and forest products (Brandt et al., 2017). Recent studies have also examined the interactions between population growth and increases in drought risk (Rohat et al., 2019).

Urbanization is yet another challenge and may exacerbate heat exposure due to the urban heat island effect (Peng et al. 2012). Notably, many recent studies were dedicated to this effect in growing cities across India (Borbora & Das, 2014; Singh, Kikon, & Verma, 2017) and China (Li, Zhang, Mirzaei, Zhang, & Zhao, 2018; Zhang, Estoque, & Murayama, 2017). As the world's largest metropolitan areas shift from the cooler high latitudes (e.g. Tokyo, Beijing, New York; Table 2) to the warmer low latitudes (e.g. Lagos, Mumbai, Karachi), more attention is given to cities in Asia and Africa. For example, a remote sensing study over Lucknow, India, found an increase of the urban heat island effect in the dense built-up areas of the city (Singh et al., 2017). In another study, the rate of population growth was found to be a good predictor of regional urban warming (Wang & Wang, 2017). Finally, considering megapolitan areas (Wang & Wang, 2017) and the future cities of unprecedented size (Table 2), the land-use change associated with urbanization might create a positive feedback with warming, that can further exacerbate population exposure to heat. Cities also contain major opportunities for climate adaptation to heat through urban planning and technologies (e.g. green roofing, air conditioning) and the increasing exposure documented here highlights an urgent need to scale up such activities. Urban vegetation has already been applied to reduce the heat island effect (Cuy & de Foy, 2012), reducing surface temperature by up to 2.5 ºC due to shading and transpiration (Shashua-Bar, Pearlmutter, & Erell, 2009).

4.1. Study limitations

The results of our analyses are only as reliable and accurate as their underlying climate and population projections. For this reason, we have used the most updated set of climate models and shared socioeconomic scenarios available. How well global climate models capture the distribution of absolute temperatures and the range of variability in these temperatures at sufficient spatial resolution is still an open question (Tokarska et al., 2020). For example, Sippel et al. (2017) have shown that simulation of temperature extremes typical of summertime heat was complexed by land surface feedbacks missing in such models. Spatial biases of absolute temperature simulations also exist, and their correction is not straightforward (Jeon, Paciorek, & Wehner, 2016), mostly due to nonlinear responses (Borodina, Fischer, & Knutti, 2017;

Sippel et al., 2016; Sippel et al., 2017). On the other hand, there is now evidence from retrospectively comparing model projections to observations that the warming shown by climate models published over the past half century were highly consistent with observations (Hausfather et al., 2020). In addition, we posit that the broad-scale spatial patterns in temperature projections – particularly the general differences among SSP scenarios in heat exposure illuminated here – are generally robust even if there is uncertainty about the precise absolute number of people exposed in a given grid cell.

Another aspect which is missing in our analysis is the calculation of heat stress. By focusing on mean absolute temperatures, we disregarded the physiological heat stress *per se*. Notably, heat stress is the product of both high temperature and high relative humidity (Matthews, 2018). In fact, a temperature of 30 °C at 100% relative humidity should have the same heat stress of 55 °C at 0% relative humidity. This large difference is important, considering that the limit of human thermoregulation is at 35 °C wet-bulb temperature (Sherwood & Huber 2010). Importantly, the identification of increased heat exposure around low latitudes in this study (Fig. 2), means that many of the sensitive regions are at tropical, humid, areas.

4.2. Implications

A major uncertainty in predicting the future of Earth's human population, and its exposure to heat, is international migration (Black et al., 2011; Gray & Wise 2016). Here we show a strong latitudinal distribution, with high exposure across Africa and India, and considerably lower exposure in cooler Eurasia and North America, with very little increase in heat exposure in Canada and Russia (Fig. 2). The latter observation is purely due to very low projected population growth in these cooler regions, and in spite of the moderately larger warming expected at higher latitudes. Climate change has been shown to drive human migration already in prehistoric times (D'Andrea, Huang, Fritz, & Anderson, 2011). Although economic, social, and political motivations dominate migration decisions today (Black et al., 2011), environmental drivers can still play a role. A model based on repeated drought- and flooding-induced migration patterns in Oklahoma, USA, in the 1930s, highlighted migration as a pathway for climate change adaptation (McLeman & Smit, 2006). In rural Pakistan, heat stress is already increasing long-term migration (Mueller, Gray, & Kosec, 2014). In Africa, a positive link between migration and temperature anomalies exists in some countries, but not in others (Rohat et al., 2019). Climate change may also influence Mexico-USA cross-border migration (Feng, Krueger, & Oppenheimer, 2010). Notably, non-migratory adaptations such as air conditioning are also expected to intensify, with further consequences on the energy sector (Davis & Gertler, 2015). Considering the increases in heat exposure hotspots identified here (Fig. 2), the conditions conducive to migration may only intensify in high climate change and population growth futures. Still, both results are not inevitable. Investments in societal measures to slow population growth, including women's rights and education access, family planning, and a general increase in life quality have proved effective (Bongaarts & O'Neill 2018). These measures, along with climate change mitigation efforts, should become a higher priority in sensitive areas such as India and Africa. Finally, our results further underscore how large reductions in greenhouse gas emissions are needed to avoid large-scale human exposure to extreme heat in the 21st century.

5. Conclusions

In this study, superposition of temperature projection maps and population projection scenario maps showed that:

(1) By 2090, high climate change and population growth scenarios show a ~5-, ~10-, and ~100–1000-fold increase in the population exposed to a mean hottest monthly temperature of 30 °C, 35 °C, and 40 °C, respectively.
(2) Globally, population growth, warming, and their interaction, are the major drivers for the increase in exposure at milder, harsher, and extreme, temperatures, respectively.
(3) Differences between population growth scenarios show that policy can potentially reduce the level of increase in exposure by up to 70%.
(4) The major driver for the increased heat exposure is the dangerous combination between global warming and population growth in already-warm cities in regions like Africa and India.

Data availability statement

All model input data used in this research are publicly available. Model output data will be uploaded to an online open database.

Author contributions

TK conceptualized the rewserach idea together with WA. WA analyzed the data together with TK. TK wrote the original draft, which was reviewed and edited by WA.

Declaration of Competing Interest

The authors declare no competing interest in the preparation of this manuscript.

Funding

Not applicable

References

Ahmadalipour, A., Moradkhani, H., Castelletti, A., & Magliocca, N. (2019). Future drought risk in Africa: Integrating vulnerability, climate change, and population growth. *Science of the Total Environment, 662*, 672–686.
Black, R., Adger, W. N., Arnell, N. W., Dercon, S., Geddes, A., & Thomas, D. (2011). The effect of environmental change on human migration. *Global Environmental Change, 21*. S3-S11.
Bongaarts, J., & O'Neill, B. C. (2018). Global warming policy: Is population left out in the cold? *Science, 361*(6403), 650–652.
Borbora, J., & Das, A. K. (2014). Summertime urban heat island study for Guwahati city. *India. Sustainable Cities and Society, 11*, 61–66.
Borodina, A., Fischer, E. M., & Knutti, R. (2017). Potential to constrain projections of hot temperature extremes. *Journal of Climate, 30*(24), 9949–9964.
Brandt, M., Rasmussen, K., Peñuelas, J., Tian, F., Schurgers, G., Verger, A., & Fensholt, R. (2017). Human population growth offsets climate-driven increase in woody vegetation in sub-Saharan Africa. *Nature Ecology & Evolution, 1*(4), 1–6.
Bulatao, R. A., Bos, E., Stephens, P. W., & Vu, M. T. (1990). *World population projections 1989*. Washington, DC, USA: World Bank.
Cohen, J. E. (2003). Human population: The next half century. *Science, 302*(5648), 1172–1175.
Cui, Y. Y., & De Foy, B. (2012). Seasonal variations of the urban heat island at the surface and the near-surface and reductions due to urban vegetation in Mexico City. *Journal of Applied Meteorology and Climatology, 51*(5), 855–868.
D'Andrea, W. J., Huang, Y., Fritz, S. C., & Anderson, N. J. (2011). Abrupt Holocene climate change as an important factor for human migration in West Greenland. *Proceedings of the National Academy of Sciences, 108*(24), 9765–9769.
Davis, L. W., & Gertler, P. J. (2015). Contribution of air conditioning adoption to future energy use under global warming. *Proceedings of the National Academy of Sciences, 112*, 5962–5967.
Diffenbaugh, N. S., & Scherer, M. (2011). Observational and model evidence of global emergence of permanent, unprecedented heat in the 20th and 21st centuries. *Climatic Change, 107*(3-4), 615–624.
Eyring, V., Bony, S., Meehl, G. A., Senior, C. A., Stevens, B., Stouffer, R. J., & Taylor, K. E. (2016). Overview of the coupled model intercomparison project phase 6 (CMIP6) experimental design and organization. Geoscientific Model Development (Online), 9 (LLNL-JRNL-736881).
Feng, S., Krueger, A. B., & Oppenheimer, M. (2010). Linkages among climate change, crop yields and Mexico–US cross-border migration. *Proceedings of the National Academy of Sciences, 107*(32), 14257–14262.
Field, C. B., Barros, V., Stocker, T. F., & Dahe, Q. (2012). *Managing the risks of extreme events and disasters to advance climate change adaptation: Special report of the intergovernmental panel on climate change*. In S. K. Allen, M. Tignor, & P. M. Midgley (Eds.). Cambridge University Press.

Frejka, T. (1981). Long-term prospects for world population growth. *Population and Development Review*, 489–511.
Gray, C., & Wise, E. (2016). Country-specific effects of climate variability on human migration. *Climatic Change, 135*(3-4), 555–568.
Hansen, J., Sato, M., & Ruedy, R. (2012). Perception of climate change. *Proceedings of the National Academy of Sciences, 109*(37). E2415-E2423.
Hausfather, Z., Drake, H. F., Abbott, T., & Schmidt, G. A. (2020). Evaluating the performance of past climate model projections. *Geophysical Research Letters, 47*(1). e2019GL085378.
Hijmans, R. J., & van Etten, J. (2014). raster: Geographic data analysis and modeling. *R Package Version, 2*, 1.
Hoegh-Guldberg, O., Jacob, D., Bindi, M., Brown, S., Camilloni, I., Diedhiou, A., & Zougmoré, R. B. (2018). Impacts of 1.5 C global warming on natural and human systems. *Global warming of 1.5 C. An IPCC Special Report.*
Hoornweg, D., & Pope, K. (2017). Population predictions for the world's largest cities in the 21st century. *Environment and Urbanization, 29*(1), 195–216.
Jeon, S., Paciorek, C. J., & Wehner, M. F. (2016). Quantile-based bias correction and uncertainty quantification of extreme event attribution statements. *Weather and Climate Extremes, 12*, 24–32.
Jones, B., & O'Neill, B. C. (2016). Spatially explicit global population scenarios consistent with the Shared Socioeconomic Pathways. *Environmental Research Letters, 11*(8), Article 084003.
Jones, B., O'Neill, B. C., McDaniel, L., McGinnis, S., Mearns, L. O., & Tebaldi, C. (2015). Future population exposure to US heat extremes. *Nature Climate Change, 5*(7), 652–655.
Jones, B., Tebaldi, C., O'Neill, B. C., Oleson, K., & Gao, J. (2018). Avoiding population exposure to heat-related extremes: Demographic change vs climate change. *Climatic Change, 146*(3-4), 423–437.
Lemon, Jim. (2006). Plotrix: A package in the red light district of R. *R-news, 6.*, 8–12.
Li, G., Zhang, X., Mirzaei, P. A., Zhang, J., & Zhao, Z. (2018). Urban heat island effect of a typical valley city in China: Responds to the global warming and rapid urbanization. *Sustainable Cities and Society, 38*, 736–745.
Matthews, T. (2018). Humid heat and climate change. *Progress in Physical Geography: Earth and Environment, 42*(3), 391–405.
McCarthy, M. P., Best, M. J., & Betts, R. A. (2010). Climate change in cities due to global warming and urban effects. *Geophysical Research Letters, 37*(9).
McLean, R., & Smit, B. (2006). Migration as an adaptation to climate change. *Climatic Change, 76*(1-2), 31–53.
Michna, Pavel, & Woods, Milton (2013). RNetCDF–A package for reading and writing NetCDF datasets. *The R Journal, 5.2*, 29–36.
Mora, C., Dousset, B., Caldwell, I. R., Powell, F. E., Geronimo, R. C., Bielecki, C. R., & Lucas, M. P. (2017). Global risk of deadly heat. *Nature Climate Change, 7*(7), 501–506.
Mueller, V., Gray, C., & Kosec, K. (2014). Heat stress increases long-term human migration in rural Pakistan. *Nature Climate Change, 4*(3), 182–185.
Pachauri, Rajendra K., Allen, Myles R., Barros, Vicente R., Broome, John, Cramer, Wolfgang, Christ, Renate, & Church, John A. (2014). *Climate change 2014: Synthesis report*. et al. Contribution of Working Groups I, II and III to the fifth assessment report of the Intergovernmental Panel on Climate Change. Ipcc
Peng, S., Piao, S., Ciais, P., Friedlingstein, P., Ottle, C., Bréon, F. M., & Myneni, R. B. (2012). Surface urban heat island across 419 global big cities. *Environmental Science & Technology, 46*(2), 696–703.
R Core Development Team. (2012). *R: A language and environment for statistical computing*. (R Foundation for Statistical Computing.
Riahi, K., Van Vuuren, D. P., Kriegler, E., Edmonds, J., O'neill, B. C., Fujimori, S., & Lutz, W. (2017). The shared socioeconomic pathways and their energy, land use, and greenhouse gas emissions implications: An overview. *Global Environmental Change, 42*, 153–168.
Robine, J. M., Cheung, S. L. K., Le Roy, S., Van Oyen, H., Griffiths, C., Michel, J. P., & Herrmann, F. R. (2008). Death toll exceeded 70,000 in Europe during the summer of 2003. *Comptes Rendus Biologies, 331*(2), 171–178.
Rohat, G., Flacke, J., Dosio, A., Dao, H., & van Maarseveen, M. (2019). Projections of human exposure to dangerous heat in African cities under multiple socioeconomic and climate scenarios. *Earth's Future, 7*(5), 528–546.
Shashua-Bar, Limor, Pearlmutter, David, & Erell, Evyatar (2009). The cooling efficiency of urban landscape strategies in a hot dry climate. *Landscape and Urban Planning, 92*(3-4), 179–186.
Sherwood, S. C., & Huber, M. (2010). An adaptability limit to climate change due to heat stress. *Proceedings of the National Academy of Sciences, 107*(21), 9552–9555.
Singh, P., Kikon, N., & Verma, P. (2017). Impact of land use change and urbanization on urban heat island in Lucknow city, Central India. A remote sensing based estimate. *Sustainable Cities and Society, 32*, 100–114.
Sippel, S., Otto, F. E., Forkel, M., Allen, M. R., Guillod, B. P., Heimann, M., & Mahecha, M. D. (2016). A novel bias correction methodology for climate impact simulations. *Earth System Dynamics, 7*(1), 71–88.
Sippel, S., Zscheischler, J., Mahecha, M. D., Orth, R., Reichstein, M., Vogel, M., & Seneviratne, S. I. (2017). Refining multi-model projections of temperature extremes by evaluation against land-atmosphere coupling diagnostics. *Earth System Dynamics, 8*(2), 387–403.
Small, C., & Cohen, J. (2004). Continental physiography, climate, and the global distribution of human population. *Current Anthropology, 45*(2), 269–277.
South, A.rworldmap (2011). A new R package for mapping global data. *R J, 3*.
Tokarska, K. B., Stolpe, M. B., Sippel, S., Fischer, E. M., Smith, C. J., Lehner, F., & Knutti, R. (2020). Past warming trend constrains future warming in CMIP6 models. *Science Advances, 6*(12), eaaz9549.
United Nations Department of Economic and Social Affairs (2019). World population prospects 2019. https://population.un.org/wpp/Publications/.
van Vuuren, D. P., & Carter, T. R. (2014). Climate and socio-economic scenarios for climate change research and assessment: Reconciling the new with the old. *Climatic Change, 122*(3), 415–429.
Vu, M. T. (1985). *World population projections 1985* (pp. 1–7). Baltimore, MD: The Johns Hopkins University press.
Wang, C., & Wang, Z. H. (2017). Projecting population growth as a dynamic measure of regional urban warming. *Sustainable Cities and Society, 32*, 357–365.
Xu, C., Kohler, T. A., Lenton, T. M., Svenning, J. C., & Scheffer, M. (2020). Future of the human climate niche. *Proceedings of the National Academy of Sciences, 117*(21), 11350–11355.
Zhang, X., Estoque, R. C., & Murayama, Y. (2017). An urban heat island study in Nanchang City, China based on land surface temperature and social-ecological variables. *Sustainable Cities and Society, 32*, 557–568.